Available online at www.sciencedirect.com
ScienceDirect
International Journal of Thermal Sciences 47 (2008) 1610–1619
International Journal of Thermal Sciences
www.elsevier.com/locate/ijts

Jet impingement heat transfer on a flat plate at a constant wall temperature

B. Sagot [a,*], G. Antonini [b], A. Christgen [a], F. Buron [a]

[a] *Laboratoire Fluide et Energétique, École Supérieure des Techniques Aéronautiques et Construction Automobile (ESTACA), 34-36 rue Victor Hugo, 92300 Levallois-Perret, France*
[b] *Laboratoire de Génie des Procédés Industriels (UMR CNRS 6067), Université de Technologie de Compiègne (UTC), BP 20529-60205, Compiegne Cedex, France*

Received 24 October 2006; received in revised form 26 September 2007; accepted 7 October 2007

Available online 30 January 2008

Abstract

Gas-to-wall heat transfer configuration for a round air jet impinging on a circular flat plate is investigated experimentally to derive an average Nusselt number correlation. The impingement plate is placed at the bottom of a large adiabatic enclosure, and its temperature is imposed, by external circulation of a coolant. The simultaneous measurements of mass flow rate and characteristic temperatures (hot jet, cold wall, enclosure outlet) permit the determination of the average wall heat transfer coefficient, through an enthalpic balance of the enclosure. The jet Reynolds number, nozzle diameter D and nozzle-to-plate distance H are varied. These experimental measurements are compared with the results of a numerical CFD modelling. Simulations under constant wall heat flux conditions are compared to local Nusselt number distributions as given by the current literature, which validates the use of the Shear Stress Transport (SST) k–ω turbulence model for this problem. Simulated Nusselt numbers obtained at a constant wall temperature are found lower than under uniform heat flux conditions. Measurements and simulation results, at a constant wall temperature, are in good agreement. An average Nusselt number correlation is proposed for jet impingement heat transfer calculations under constant wall temperature conditions, as a function of the jet Reynolds number Re_j ($10\,000 \leqslant Re_j \leqslant 30\,000$), the geometrical parameters R/D, H/D ($3 \leqslant R/D \leqslant 10$; $2 \leqslant H/D \leqslant 6$), and the dimensionless viscosity ratio μ_j/μ_w ($1.1 \leqslant \mu_j/\mu_w \leqslant 1.4$).

Keywords: Jet impingement; Heat transfer; Nusselt number; Experimental correlation; Constant wall temperature; Viscosity correction ratio; SST k–ω

1. Introduction

Wall impinging jet flows are widely used in engineering applications due to their high heat transfer performances. These configurations are encountered in many industrial areas where an efficient heat transfer is needed, in particular for air blast cooling of electronic components or turbine blades and drying applications. Jet cooling is used in various geometrical configurations implementing either a single injector or several parallel jets generated by a multiperforated plate. It can also be associated with a tangential sweeping flow parallel to the cooled surface. This convective heat transfer configuration is used for its high local transfer coefficients nearby the stagnation point. Accordingly, the current literature mainly reports jet impingement configurations on circular plane plates with $R/D \leqslant 5$ where R/D is the ratio of the plate radius R to the injection diameter D.

Applications can be separated in two categories: heating/cooling configurations either at a constant wall temperature (quench cooling) or at a uniform wall heat flux (electronic components cooling). In this research field a lot of work has been already done including theoretical approaches, experimental investigations or numerical simulations. It is remarkable that the majority of the experiments reported in the literature refers to uniform wall heat flux configurations. Probably, this is due to the experimental methodology based on infra-red thermography, widely used for heat transfer characterisation and involving an electrically heated plate impacted by a cooling jet, permitting the plate surface temperature field measurement, from which the local heat transfer coefficients can be determined [1–5].

* Corresponding author.
E-mail address: bsagot@estaca.fr (B. Sagot).

1290-0729/$ – see front matter
doi:10.1016/j.ijthermalsci.2007.10.020

Nomenclature

C_p	specific heat	$J\,kg^{-1}\,K^{-1}$
D	nozzle diameter	m
D_v	diameter of the enclosure	m
D_ω	cross-diffusion term	$kg\,m^{-3}\,s^{-2}$
e	nozzle thickness	m
e_s	specific total energy	$J\,kg^{-1}$
G_k	production term of turbulent kinetic energy	$kg\,m^{-1}\,s^{-3}$
G_ω	production term of specific dissipation rate	$kg\,m^{-3}\,s^{-2}$
H	nozzle-to-plate distance	m
h	local heat transfer coefficient	$W\,m^{-2}\,K^{-1}$
$\bar{h}$	average heat transfer coefficient	$W\,m^{-2}\,K^{-1}$
h_s	specific enthalpy	$J\,kg^{-1}$
k	turbulent specific kinetic energy	$m^2\,s^{-2}$
$\dot{m}_g$	gas mass flow rate	$kg\,s^{-1}$
Nu	Nusselt number	(–)
Nu_φ	local Nusselt number at a constant wall heat flux	(–)
Nu_T	local Nusselt number at a constant wall temperature	(–)
$\overline{Nu}_\varphi$	average Nusselt number at a constant wall heat flux	(–)
$\overline{Nu}_T$	average Nusselt number at a constant wall temperature	(–)
p	static pressure	Pa
Pr	Prandtl number	(–)
Q_v	air flow rate	$m^{-3}\,s^{-1}$
R	plate radius	m
r	radial coordinate	m
Re_j	jet Reynolds number	(–)
T	temperature	K
Tu	turbulence intensity	%
u_i, u_j	velocity components	$m\,s^{-1}$
U_j	average gas velocity at nozzle exit	$m\,s^{-1}$
v	velocity	$m\,s^{-1}$
x	nozzle chamfer thickness	m
Y_k	dissipation term of specific turbulent kinetic energy	$kg\,m^{-1}\,s^{-3}$
Y_ω	dissipation term of specific dissipation rate	$kg\,m^{-3}\,s^{-2}$
z	vertical distance from the nozzle exit	m

Greek symbols

α, β, γ	non-dimensional constants in Eq. (10)	(–)
Φ	heat flux W	
Γ_k	effective diffusivities of k	$kg\,m^{-1}\,s^{-1}$
Γ_ω	effective diffusivities of ω	$kg\,m^{-1}\,s^{-1}$
φ	heat flux density	$W\,m^{-2}$
λ	thermal conductivity	$W\,m^{-1}\,K^{-1}$
μ	dynamic viscosity	$kg\,m^{-1}\,s^{-1}$
ρ	density	$kg\,m^{-3}$
ω	specific dissipation rate	s^{-1}

Subscripts

aw	adiabatic
eff	effective
exp	experimental
g	gas
j	jet
o	outlet
t	turbulent
w	wall
∞	free-stream conditions

In using this experimental procedure an uncertainty on the gas/wall heat transfer coefficient definition results from the lack of reference temperature. Under constant flux conditions it is common to introduce an adiabatic wall temperature which defines the local heat transfer coefficient as:

$$h = \varphi/(T_w - T_{\mathrm{aw}}) \tag{1}$$

where φ is the convective wall flux density, T_w the wall temperature and T_{aw} the adiabatic wall temperature obtained without cooling or heating the plate [2]. The associated local Nusselt number at a constant wall heat flux is noted as Nu_φ.

In an imposed temperature approach two reference temperatures have to be fixed: the jet temperature T_j and the wall temperature T_w. Under these conditions, the convective flux density is written as:

$$\varphi = h(T_j - T_w) \tag{2}$$

and the corresponding local Nusselt number $Nu_T(r)$ can be defined as:

$$Nu_T(r) = h(r)D/\lambda_g \tag{3}$$

with $h(r)$ the local convective heat transfer coefficient, D the nozzle diameter, and λ_g the gas thermal conductivity. Thus, the heat flux $\Phi(R)$ on a circular plate of radius R is written as:

$$\Phi(R) = \int_0^R \varphi(r) 2\pi r \,\mathrm{d}r \tag{4}$$

The average convective wall heat transfer coefficient is consequently defined as:

$$\bar{h}(R) = \frac{1}{\pi R^2}\frac{\Phi(R)}{T_j - T_w} \tag{5}$$

and the corresponding average Nusselt number as:

$$\overline{Nu}_T(R) = \frac{\bar{h}(R)D}{\lambda_g} \tag{6}$$

Finally a jet Reynolds number based on the nozzle outlet conditions can be defined as:

$$Re_j = \frac{\rho_g U_j D}{\mu_g} = \frac{4\dot{m}_{\mathrm{g}}}{\mu_g \pi D} \tag{7}$$

with $\dot{m}_g$ the imposed gas mass flow rate, U_j the jet average velocity at the nozzle exit, μ_g the gas dynamic viscosity, ρ_g its density, evaluated at the jet temperature. Furthermore, the nozzle-to-plate distance is taken into account [1] by using a dimensionless parameter H/D which is the ratio of the distance H between the nozzle and the impacted wall to the nozzle diameter D. The dimensionless radial position on the plate is noted as r/D.

The effect of turbulence intensity in the free stream jet impinging on a wall has been identified [6] as a parameter influencing the forced convective heat transfer at the stagnation point. However, this turbulence intensity Tu is measured along the centerline of the free jet without the impingement plate. For the high values of H/D (between 2 and 6) used in this study, it seems more relevant to introduce the turbulence intensity at the nozzle exit, equivalent for both free and impacting jet configurations.

The present work is based on experimental measurements of gas-to-wall heat transfer, as a function of the jet Reynolds number Re_j, geometrical parameters H/D and R/D, for $3 \leqslant R/D \leqslant 10$ and $2 \leqslant H/D \leqslant 6$, at a uniform wall temperature, with an experimental turbulence intensity at the nozzle exit varying between 4.3 and 7.3%. From these results, we propose an average Nusselt number correlation, which is compared with a numerical CFD modelling. This numerical study is carried out with a Shear Stress Transport (SST) k–ω turbulence model.

2. Experimental setup and methodology

The experimental setup implementing a hot gas jet impacting on a cold wall is presented schematically in Fig. 1. The radius of the impacted circular plate is $R = 24$ mm. The jet enters into a PMMA cylindrical vessel with a thickness of 3 mm, height of 200 mm and an inner diameter $D_v = 154$ mm. The enclosure/plate radius ratio is 3.2 which minimises any possible jet confinement effects. The enclosure gas outlet consists in a 33 mm diameter tube located on the top of the enclosure (Fig. 1). The large values of the enclosure diameter and height make it possible to consider the impinging flow as axisymmetric.

In this experimentation, the steady heat flux Φ exchanged between the jet and the plate is determined by a heat balance between the inlet and outlet of the enclosure. In this setup the heat losses have been minimised: the average temperature inside the vessel is close to the ambient temperature. Moreover, the low conductivity plastic enclosure is glass wool insulated. Finally, the upper part of the water cooled block acting as the impacted plate (Fig. 1) is contactless flush-mounted with the enclosure bottom to avoid cold bridges. This procedure permits to consider the enclosure as adiabatic under the test conditions. This was checked by replacing the cooling impinging block by an insulant wall, and by measuring the gas temperature variation between the inlet and outlet of the enclosure. This variation always remained lower than the temperature measurement error.

By increasing r/D the free convection effects have a growing relative magnitude compared to the forced convection. This is due to the reduction of the local forced convection heat transfer coefficients while the distance from the stagnation point increases. The chosen configuration of a downwards flowing hot gas jet onto a cold plate has a positive vertical temperature surface gradient which limits detrimental free convection effects, currently observed in conventional experimental arrangements using electrically heated plates.

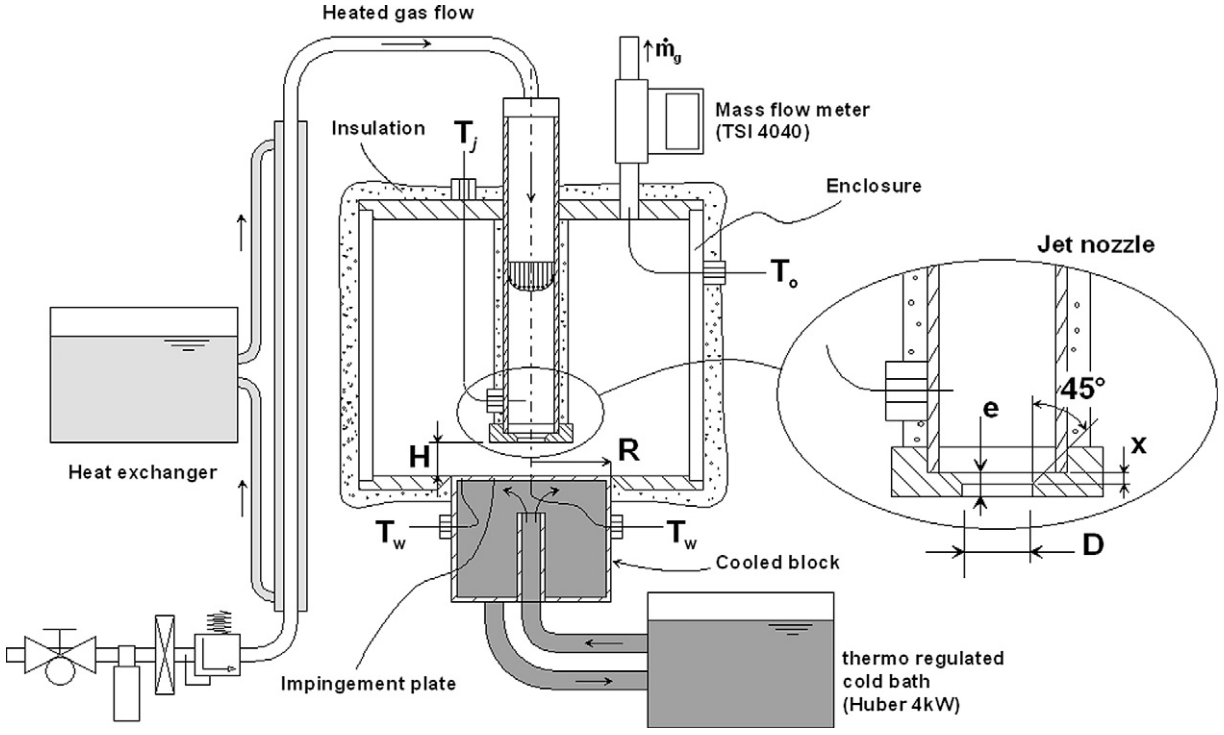

Fig. 1. Schematic of the experimental setup.

The gas flows through a 200 mm long thermally insulated pipe with a large inner diameter (17 mm) in order to minimise the pressure drop of the injection device, and to obtain a fully developed flow at the nozzle inlet. This tube ends in an interchangeable nozzle that allows a variation of the ratio R/D. The nozzle restriction geometry accelerates the flow, thus generating a flat velocity profile. The nozzle diameter varies between 2.4 and 8 mm, with a constant thickness $e = 2$ mm (Fig. 1), with a pressure drop limited by a 45° angle chamfer, with a chamfer thickness $x = 1$ mm (Fig. 1). Furthermore, the change of the nozzle-to-plate distance permits the adjustment of the H/D parameter.

The jet Reynolds number Re_j is fixed by adjusting the gas flow rate. For a given nozzle, this flow rate is measured using a double hot wire anemometer (TSI 4040) which is coupled with pressure and temperature measurements to determine the gas mass flow rate. The hot jet temperature T_j and gas outlet temperature T_o are measured with type K thermocouples, respectively located close to the nozzle and at the gas enclosure exit.

Velocity and turbulence intensity measurements at the nozzle exit were carried out using a Dantec, two components, LDA system, in a free jet configuration, where the enclosure and impingement plate were removed.

A controlled air flow rate is supplied by a compressed air unit, de-oiled, dried, and heated in a coaxial exchanger ensuring a stable jet temperature. During the experiments the gas jet temperature T_j was fixed between 40 and 65 °C depending on the Reynolds number. In the operating conditions of this study, the heat flux exchanged between the hot jet and the cold plate varied between 10 and 60 W.

The temperature of the cooled block supporting the impingement plate (Fig. 1) is fixed by an internal water circulation. A high flow rate of a cooling fluid with a regulated temperature (refrigerating unit Huber 4 kW, −55/+100 °C, stability: 0.02 °C) is used to maintain a fixed and uniform temperature on the impingement plate. Thus, under test conditions, the extracted heat flux remained lower than 1.5% of the cryostat capacity. The impinging surface is an aluminum plate (thickness 3 mm, conductivity 210 $\mathrm{W\,m^{-1}\,K^{-1}}$). Two thermocouples (Fig. 1) are inserted one millimetre under the impact surface, below the stagnation point and at the plate border. Measurements given by these thermocouples confirmed the surface temperature uniformity, with a maximum temperature deviation of approximately 0.5° between the stagnation point and the plate border. A correction taking into account the conductive resistance of the plate is used to determine the effective wall surface temperature T_w. Due to the low thermal resistance of the cooled plate this correction remains lower than 0.2 °C. During the experiments the wall temperature remained close to $T_w = 4$ °C.

This experimental procedure, though not leading to the local heat flux determination, permits the determination of the average wall heat transfer coefficient, by the simultaneous measurements of T_j, T_o, T_w and mass flow rate $\dot{m}_g$. The convective heat flux $\Phi(R)$ on the circular plate of radius R has been experimentally determined with:

$$\Phi(R) = \dot{m}_g C_p (T_j - T_o) \tag{8}$$

The experimental average convective wall heat transfer coefficient was then determined by using:

$$\bar{h}(R) = \frac{\dot{m}_g C_p}{\pi R^2} \frac{T_j - T_o}{T_j - T_w} \tag{9}$$

$\overline{Nu}_T$ is then evaluated using (6), with the gas thermal conductivity λ_g being evaluated at the average gas temperature $(T_j + T_o)/2$.

3. Experimental results

For the average Nusselt numbers determination, we use the experimental setup described previously (Fig. 1). Experimental results were obtained for various jet Reynolds numbers, for $2 \leqslant H/D \leqslant 6$ and $2 \leqslant R/D \leqslant 10$. The uncertainty on the average Nusselt number $\overline{Nu}_T$ due to errors on temperature measurements, mass flow measurements, and thermal losses has been investigated. The heat transfer experiments reported here were repeated between three and ten times, depending on the relative standard deviation of the experimental results. All the measured values were within ±5% of the average value.

Fig. 2 shows the variation of the average Nusselt number $\overline{Nu}_T$ with the R/D parameter, for $H/D = 2$ and $10\,000 \leqslant Re_j \leqslant 30\,000$, with ±5% vertical error bars. The average Nusselt number $\overline{Nu}_T$ decreases with the Reynolds number, and $\overline{Nu}_T$ decreases globally monotonously for $R/D > 3$ and for a given Reynolds number.

Fig. 3 shows the dependence of the experimental average Nusselt number $\overline{Nu}_T$ on H/D. The results are presented for two intermediate values $R/D = 4$ and $R/D = 6$. We observe a small dependence of $\overline{Nu}_T$ on the dimensionless nozzle-to-plate distance H/D.

As the turbulence intensity of the jet can be a relevant parameter for the heat transfer efficiency, an experimental determination of this parameter at the nozzle exit has been carried out. The turbulence intensity Tu, dependent on the chosen nozzle geometry (Fig. 1), is measured along the centerline of a free jet, in absence of the enclosure and impinging plate. These measurements have been carried out using a two components LDA

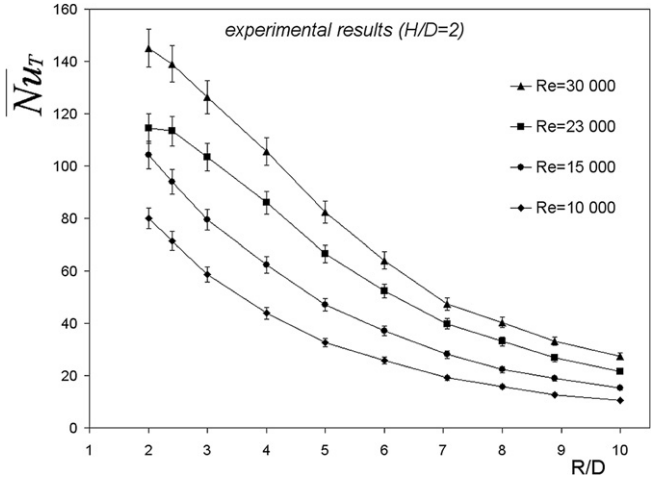

Fig. 2. Experimental average Nusselt number for $H/D = 2$ and various Reynolds numbers.

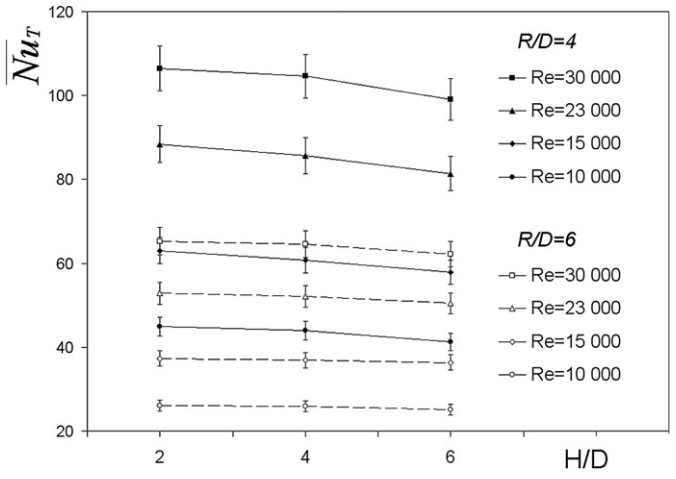

Fig. 3. Dependence of experimental average Nusselt number on H/D for $R/D = 4$, $R/D = 6$ and various Reynolds numbers.

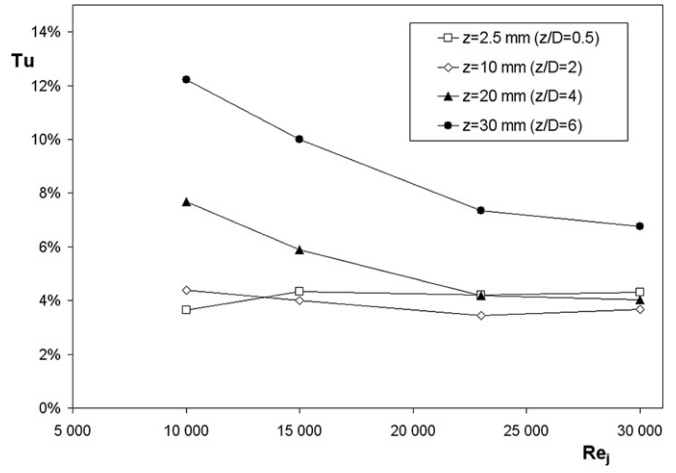

Fig. 4. Dependence of turbulence intensity Tu on jet Reynolds number, for $D = 4.8$ mm ($R/D = 5$), and various z.

system, for nozzle diameters ranging from 2.4 to 8 mm, corresponding to R/D values between 3 and 10, and to z/D values of 0.5, 2, 4 and 6. In this configuration, z is the distance between the jet nozzle exit and the measurement point along the centerline of the free jet.

The following Fig. 4 shows the results obtained for the turbulence intensity Tu as a function of the jet Reynolds number Re_j, for a nozzle diameter of 4.8 mm (corresponding to $R/D = 5$), and for various distances z between the nozzle exit and the measurement point.

For a given jet Reynolds number, the turbulence intensity in this free jet development configuration increases along the axis with the distance from the nozzle exit. However, it is observed that at short distances from the nozzle exit, the turbulence intensity Tu does not depend on z, and is independent on the jet Reynolds number. This result is confirmed with measurements for nozzle diameters of 2.4 and 8 mm (corresponding to $R/D = 3$ and $R/D = 10$). Turbulence intensity measured at the nozzle exit (corresponding to $z/D = 0.5$) ranges between 4.3 and 7.3%, for the prescribed R/D values, and for Reynolds numbers Re_j varying from 10 000 to 30 000.

Thus, in this jet to plate heat transfer study, the turbulence intensity at the nozzle exit can be considered as constant, only depending on the nozzle geometrical characteristics, with no dependence on both the jet Reynolds number and the geometrical parameters R/D, H/D.

4. Correlation

In the current literature concerning the heat transfer to a wall impinged by circular [6] or rectangular [7] jets, or to a cylinder placed in a uniform flow [8], the dimensionless group $(Nu/Re^{1/2})$ is expressed as a function of the parameter $Tu\,Re^{1/2}$, in the form:

$$Nu/Re^{1/2} = \alpha + \beta\left(Tu\,Re^{1/2}\right) - \gamma\left(Tu\,Re^{1/2}\right)^2 \tag{10}$$

where α, β and γ are specified constants.

In these studies, the artificially induced turbulence intensity is obtained by modifying the upstream flow (using smooth flow contraction, wire grids, ...), while preserving the same Reynolds number Re_j. In our study, heat transfer measurements were carried out with the same nozzle geometry, and LDA measurements have shown that the nozzle outlet turbulence intensity could be considered as constant on the whole range of the studied parameters. Thus, the turbulence intensity at the nozzle outlet Tu does not need to be introduced here as an independent parameter.

Then, a correlation by least squares method of all experimental results obtained at a constant wall temperature and for varied jet impaction conditions (Re_j, R/D, H/D) is proposed in the form:

$$\overline{Nu}_{T,\exp} = 0.0623 Re_j^{0.8}\left[1 - 0.168\left(\frac{R}{D}\right) + 0.008\left(\frac{R}{D}\right)^2\right] \times \left(\frac{H}{D}\right)^{-0.037} \tag{11}$$

for $10\,000 \leqslant Re_j \leqslant 30\,000$, $3 \leqslant R/D \leqslant 10$ and $2 \leqslant H/D \leqslant 6$.

The correlation (11) based on our experimental results is valid for $10\,000 \leqslant Re_j \leqslant 30\,000$, as shown in Fig. 5: the average relative deviation of the experimental values to this correlation (11) is 3%. For $3 \leqslant R/D \leqslant 10$ a maximum deviation of 8% is obtained. This deviation reaches 14% for values of $R/D = 2$ which shows the limitation of the Nusselt number correlation for low R/D values.

5. Numerical approach

Many local wall Nusselt number correlations at a fixed radial position, including the stagnation point, are available in the current literature [1,9]. However, these results for jet impingement heat transfer are obtained under constant wall heat flux conditions. Recent studies [10] have shown that the heat transfer simulation of this turbulent flow configuration is quite complex. Indeed, the selected turbulence model has to be able to describe the jet development, its impact, the laminar/turbulent transition which takes place downstream the stagnation point, as well as the boundary layer development along the plate. A comparison between the results obtained by using different turbulence

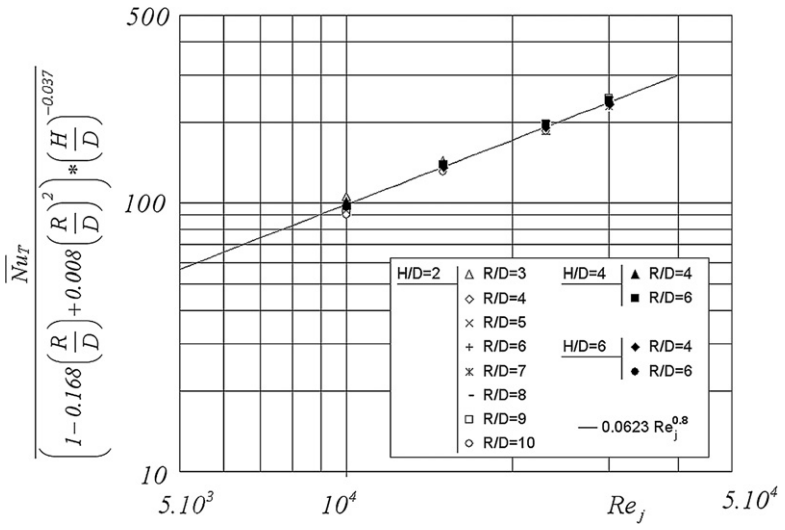

Fig. 5. Experimental average heat transfer as a function of Reynolds number, for various geometrical parameters.

models [11,12] has shown that k–ε type models are not appropriated to determine the local wall Nusselt number for this kind of flow configuration. Thus, this confrontation is extended in the present work by using the Realisable k–ε, RNG k–ε, k–ω, and SST k–ω turbulence models for the following conditions: $Re_j = 23\,000$, $H/D = 2$ under constant heat flux conditions on the impaction plate.

The determination of Nu_φ depends on the experimental evaluation of the adiabatic wall temperature T_{aw} which seems to be difficult [2]. Numerically, this procedure is replaced by a simulation under adiabatic conditions to find in a first step the adiabatic wall temperature $T_{\mathrm{aw}}(r)$. The second step is a recalculation under prescribed flux φ which leads to the wall temperature repartition $T_w(r)$. Finally, the local heat transfer coefficient is determined to derive the local wall Nusselt number distribution by using:

$$Nu_\varphi(r) = \frac{\varphi D}{\lambda_g(T_w(r) - T_{\mathrm{aw}}(r))} \tag{12}$$

Based on available literature [2,3,13] the numerical and experimental results are compared. A 2D axi-symmetric analysis of fluid flow and heat transfer was carried out using CFD software FLUENT 6.2. A rectangular mesh with grid adaptation for $y+ < 1$ at adjacent wall region has been used to resolve the laminar sub-layer. Dimensions used for the simulation are those defined on Fig. 1 (PMMA cylindrical vessel of height 200 mm, and inner diameter $D_v = 154$ mm). The geometry of the nozzle and of its supporting tube, which were described previously (nozzle diameter and thickness, chamfer angle and thickness, …), were taken into account in the grid definition, which consisted in a total of around 55 000 rectangular cells. Because of the large range of geometrical parameters (H/D, R/D) utilised in this study, an automatic mesh generation procedure was used. The boundary conditions taken into account in simulations were adiabatic wall conditions, except on the impingement plate (48 mm diameter) with imposed temperature ($T_w = 4\,^\circ\mathrm{C}$). The inlet condition was an imposed mass flow condition, with a flow rate adjusted according to the prescribed Reynolds number, with an imposed temperature. The turbulence intensity has been fixed at a constant value of 4%, and the dissipation rate was calculated from the hydraulic diameter associated with an established flow condition. Because of the axi-symmetric 2D chosen configuration, the 33 mm diameter outlet has been represented by an annular slot of equivalent section, with a prescribed pressure condition.

This simulated flow is governed by compressible form of the Reynolds-averaged Navier–Stokes (RANS) equations and by the additional equations describing the transport of other scalar properties, neglecting viscous dissipation in the energy transport equation (15).

They may be written in Cartesian tensor notations as:

$$\frac{\partial \rho}{\partial t} + \frac{\partial}{\partial x_i}(\rho u_i) = 0 \tag{13}$$

$$\begin{aligned}\frac{\partial(\rho u_i)}{\partial t} + \frac{\partial(\rho u_i u_j)}{\partial x_j} &= -\frac{\partial p}{\partial x_i} + \frac{\partial}{\partial x_j}\left[\mu\left(\frac{\partial u_i}{\partial x_j} + \frac{\partial u_j}{\partial x_i} - \frac{2}{3}\delta_{ij}\frac{\partial u_l}{\partial x_l}\right)\right] \\ &\quad + \frac{\partial}{\partial x_j}(-\rho\overline{u_i' u_j'})\end{aligned} \tag{14}$$

where μ is the gas dynamic viscosity. The dependence of μ on temperature has been taken into account by utilisation of a Sutherland law.

$$\frac{\partial(\rho e_s)}{\partial t} + \frac{\partial}{\partial x_i}\left[u_i(\rho e_s + p)\right] = \frac{\partial}{\partial x_j}\left[\lambda_{\mathrm{eff}}\frac{\partial T}{\partial x_i}\right]$$

with

$$e_s = h_s - \frac{p}{\rho} + \frac{v^2}{2} \tag{15}$$

Shear stress transport (SST) turbulence models combine the advantages of the k–ε and k–ω models, with a blending function that activates the k–ε model in the core region of the flow, and shifts to the k–ω model for the near-wall region treatment. This model has been used for the simulation of flow situations

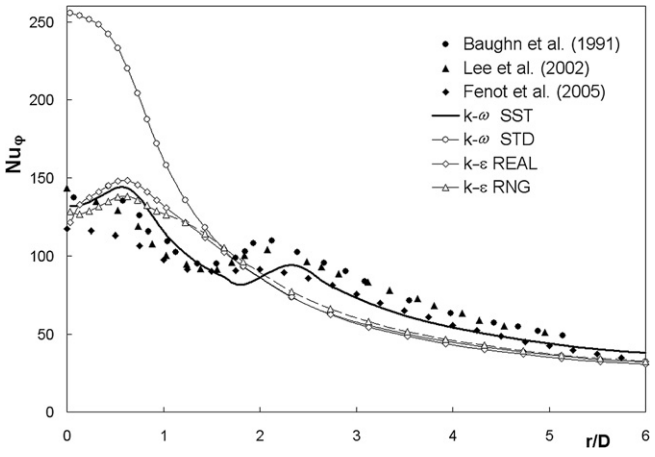

Fig. 6. Local Nusselt numbers Nu_φ obtained with various turbulence models compared to experimental literature results for $Re_j = 23\,000$ and $H/D = 2$.

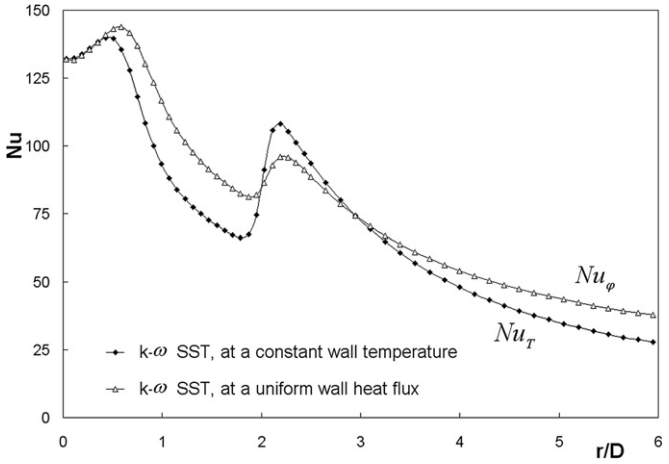

Fig. 7. Local Nusselt numbers distribution for $Re_j = 23\,000$ and $H/D = 2$.

where core and wall bounded regions need both to be modelled with good accuracy, and gave satisfactory results [11,12].

The transport equations for SST k–ω are:

$$\frac{\partial(\rho k)}{\partial t} + \frac{\partial(\rho k u_i)}{\partial x_i} = \frac{\partial}{\partial x_j}\left(\Gamma_k \frac{\partial k}{\partial x_j}\right) + G_k - Y_k \tag{16}$$

$$\frac{\partial(\rho \omega)}{\partial t} + \frac{\partial(\rho \omega u_i)}{\partial x_i} = \frac{\partial}{\partial x_j}\left(\Gamma_\omega \frac{\partial \omega}{\partial x_j}\right) + G_\omega - Y_\omega + D_\omega \tag{17}$$

In Eqs. (16) and (17), G_k represents the generation of the turbulent kinetic energy k, due to mean velocity gradients, and G_ω represents the generation of the specific dissipation rate ω. Γ_k and Γ_ω represent the effective diffusivities of k and ω, respectively. Y_k and Y_ω represents the dissipation of k and ω due to turbulence. D_ω is a cross-diffusion term [14]. The effective conductivity $\lambda_{\text{eff}} = \lambda + \lambda_t$ in the energy conservation equation (15) takes into account the turbulent thermal conductivity λ_t defined as:

$$\lambda_t = \frac{c_p \mu_t}{Pr_t} \tag{18}$$

Previous studies [11,12] showed that the SST predicts well the near-wall turbulence compared to other eddy viscosity models. This is essential for an accurate prediction of the turbulent wall heat transfer and the present confrontation confirms the quality of the SST k–ω model for this kind of flow configuration. The SST k–ω describes correctly the local Nusselt number distribution as found in imposed flux experiments by Fenot et al. [2], Lee et al. [3], and Baughn et al. [13].

These experiments [2,3,13] were realised in the same conditions with a jet issuing from a tube having a well established velocity profile. Fig. 6 shows the good confrontation between SST simulated and experimental literature Nusselt numbers at the stagnation point and also for the prediction of the secondary maximum position around $r/D = 2$. The Nusselt number decrease, obtained numerically for $r/D > 3$, is in good accordance with the experimental data. Thus, this model has been chosen for the following numerical impingement jet calculations.

In the available literature for smooth tubes, heat transfer coefficient correlations are different for uniform heat flux and constant temperature boundary conditions [15]. The SST k–ω turbulence model was applied to the reference case of $Re_j = 23\,000$, $H/D = 2$ at a constant wall temperature. Nusselt numbers, Nu_φ at a uniform heat flux and Nu_T at a constant temperature, are compared as shown in Fig. 7. The imposed flux value is taken as the average wall flux resulting from the imposed temperature calculation, to get aerodynamic and thermal conditions as close as possible for both calculations.

This confrontation shows that:

- The Nusselt number at the stagnation point does not depend on the imposed wall thermal boundary condition.
- The second peak in the Nusselt number distribution is obtained for the same value $r/D = 2.2$.
- The deviation between the local Nusselt numbers Nu_φ and Nu_T increases for $r/D > 3$ ($Nu_\varphi > Nu_T$).

To study the validity of the fixed temperature condition imposed on the impingement plate, coupled calculations were realised, taking into account conduction within the aluminum plate. In these calculations, the temperature was imposed on the wetted lower face of the aluminum plate, in accordance with the high forced flow rate of the cooling liquid, imposed by the cryostat. As an example, for $R/D = 5$, $H/D = 2$, and $Re = 23\,000$, the difference between the average Nusselt numbers obtained at a fixed impingement plate surface temperature, and for the corresponding coupled calculation is around 0.05%, showing that the impinging surface can be considered at a uniform temperature.

In the chosen experimental configuration, the confinement effects are limited by the ratio between the enclosure and impingement plate diameters (see Discussion, paragraph 2). To check the absence of confinement effects on heat transfer, a calculation on the reference case ($R/D = 5$, $H/D = 2$, and $Re = 23\,000$) has been realised, by increasing the radius of the enclosure diameter by a factor of 2. This calculation leads to an average Nusselt number of 66.28, to be compared with a value of 66.31 in the reference case. This corresponds to a relative variation of 0.05%. This numerical result confirms that the

enclosure diameter chosen in the experimental set-up is large enough to neglect any confinement effect on the mean heat transfer. The provided correlation (11) is thus valid in the absence of enclosure.

6. Discussion

The experimental average Nusselt number variations as a function of R/D are reported in Fig. 8, for the reference case $Re_j = 23\,000$ and $H/D = 2$. Our measurements have been obtained under temperature imposed conditions, and the corresponding numerical results, obtained with the SST k–ω turbulence model, are also reported in Fig. 8.

The experimental results available in the literature are generally obtained with imposed flux boundary conditions, giving the local Nusselt number repartition on the impingement plate [2,3,13]. From these results, we have realised a spatial averaging of the local Nusselt number distributions, using Eqs. (4) and (5). Gao et al. [4] provided the average Nusselt number distribution over a flat plate, and their results are reported in Fig. 8 together with the other results from the literature. The corresponding simulation was then carried out with imposed flux conditions, and with the SST k–ω turbulence model. These results are also reported in Fig. 8.

The confrontation of these experimental and numerical results obtained with both temperature and flux imposed conditions shows that:

- The average Nusselt number $\overline{Nu}_\varphi$ is always higher than $\overline{Nu}_T$. For instance, for the reference case $Re_j = 23\,000$, $H/D = 2$ and for $R/D = 6$ the average Nusselt numbers are $\overline{Nu}_T = 52.4$ and $\overline{Nu}_\varphi = 59.2$, corresponding to a relative deviation of 13%.
- Simulations carried out with imposed flux conditions and with the SST k–ω turbulence model show a good agreement with $\overline{Nu}_\varphi$ values resulting from spatial averaging of experimental measurements from the literature, for R/D values starting from $R/D = 2$.
- In the same way, simulations carried out with temperature imposed conditions are in good concordance with our experimental measurements. Within the R/D range of the suggested correlation (11) ($3 \leqslant R/D \leqslant 10$), the average relative deviation is 5%, with a maximum relative deviation of 12%, obtained for $R/D = 10$.

All the experimental configurations have been simulated with the SST k–ω turbulence model, for different Re_j, R/D and H/D values. The capacity of this turbulence model to describe correctly jet impingement heat transfer has been detailed in paragraph 5. The numerical results are compared in Fig. 9 with the results provided by the experimental correlation (11). The resulting average relative deviation is 7%.

In our experimental conditions, the turbulence intensity has been found close to 4% (Fig. 4). The influence of the turbulence intensity at the nozzle exit on the heat transfer was tested numerically. We carried out simulations for $R/D = 5$, $H/D = 2$, $H/D = 6$, with $Re_j = 10\,000$, $15\,000$, $23\,000$ and $30\,000$. Various values of turbulence intensity at the tube inlet were tested (2, 4, 6 and 8%) and the resulting turbulence intensity at the nozzle exit has been found to vary between 3.5 and 12.5%. Under these conditions, the relative variations of the average Nusselt number do not exceed 0.5%. Thus, the proposed correlation (11) is valid with an accuracy of 0.5%, whatever the value of the turbulence intensity at the nozzle exit may be, varying between 3.5 and 12.5%.

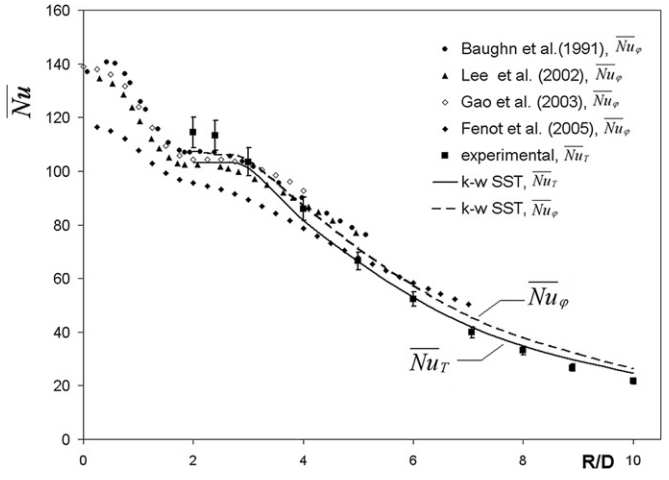

Fig. 8. Confrontation of experimental and numerical (SST k–ω model) average Nusselt number for $Re_j = 23\,000$ and $H/D = 2$.

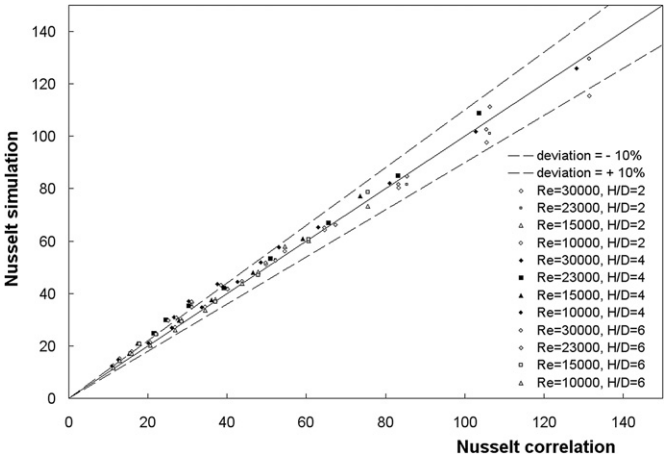

Fig. 9. Confrontation of average Nusselt numbers $\overline{Nu}_T$ between numerical values and the applied correlation (11) for different R/D, H/D and Re_j.

The film heat transfer coefficient is directly influenced by the temperature dependence of the gas viscosity. In some classical configurations of flow past thin flat plates, cylinders or spheres, it is well recognised that the Nusselt number should depend on the viscosity ratio $(\mu_\infty/\mu_w)^n$, with $n = 0.25$ [15], valid for $0.26 < \mu_\infty/\mu_w < 3.5$. The corresponding correction in pipe flow utilises a value of $n = 0.14$, with a viscosity ratio based on the free stream and the wall temperatures [16]. The resulting classical correction is expressed as:

$$\frac{Nu}{Nu_0} = (\mu_\infty/\mu_w)^n \tag{19}$$

with Nu_0 the Nusselt number obtained when the dependence of viscosity on temperature can be neglected ($\mu_\infty/\mu_w \sim 1$), generally valid for low temperature differences between the free stream and the wall. We thus seek a correlation written in the form:

$$\overline{Nu}_T = \overline{Nu}_{T,0}\left(\frac{\mu_j}{\mu_w}\right)^n \tag{20}$$

with $\overline{Nu}_{T,0}$ depending only on the geometrical parameters and on the Reynolds number. In the experimental conditions, μ_j/μ_w was close to 1.14. Thus, between our prescribed experimental conditions and for another gas-to-wall temperature difference, we should have:

$$\overline{Nu}_T = \overline{Nu}_{T,\exp}\frac{(\mu_j/\mu_w)^n}{(\mu_j/\mu_w)^n_{\exp}} \tag{21}$$

with $\overline{Nu}_{T,\exp}$ given by correlation (11).

To determine the value of n, a parametric study of the influence of the viscosity ratio μ_j/μ_w was realised numerically, by minimisation by the least squares method on a large set of simulations corresponding to the range of parameters $10\,000 \leqslant Re_j \leqslant 30\,000$, $3 \leqslant R/D \leqslant 10$, $2 \leqslant H/D \leqslant 6$. The viscosity ratio $\mu_j(T_j)/\mu_w(T_w)$ has been varied between 1.1 and 1.4, corresponding to a temperature difference $T_j - T_w$, between the air jet and the wall, ranging from 40 to 115 °C. For low temperature differences between the jet and the wall, the effects of gas compressibility, which modify the local temperature distribution in the impact zone, have also an influence on heat transfer. We have verified that the compression effects at the stagnation point can be neglected, for a temperature difference $T_j - T_w$ higher than 30 °C.

For these ranges of parameters, a least-square minimisation has lead to an optimal value of $n = 1/4$. This value ensures a maximum relative deviation of 4% between the simulated and the corrected Nusselt number $\overline{Nu}_T$ given by (21), with an average deviation of 1%. However, this correction taking into account the gas-to-wall temperature difference does not exceed 9% in our experimental measurements.

The proposed correlation, for constant wall temperature, can then be written as:

$$\overline{Nu}_T = 0.0603 Re_j^{0.8}\left[1 - 0.168\left(\frac{R}{D}\right) + 0.008\left(\frac{R}{D}\right)^2\right] \times \left(\frac{H}{D}\right)^{-0.037}\left(\frac{\mu_j}{\mu_w}\right)^{0.25} \tag{22}$$

for $10\,000 \leqslant Re_j \leqslant 30\,000$, $3 \leqslant R/D \leqslant 10$ and $2 \leqslant H/D \leqslant 6$.

7. Conclusion

Heat transfer for a hot jet impinging on a cold circular flat plate configuration has been investigated experimentally at a constant wall temperature. Experimental measurements were used to derive an average Nusselt number $\overline{Nu}_T$ correlation in the jet Reynolds number range $10\,000 \leqslant Re_j \leqslant 30\,000$ and for various geometrical parameters $3 \leqslant R/D \leqslant 10$ and $2 \leqslant H/D \leqslant 6$.

Most of the experimental results available in the current literature have been obtained under constant wall heat flux conditions. Thus, in a first step, a CFD study under imposed heat flux boundary conditions has been carried out to validate a numerical approach using various turbulence models. Local Nusselt number $Nu_\varphi(r/D)$ distributions as given by the SST k–ω turbulence model showed good agreement with the current literature for the reference case $Re_j = 23\,000$ and $H/D = 2$, for predictions of both stagnation point Nusselt number and secondary maximum position of the radial Nusselt number distribution.

This numerical modelling has then been applied at a constant wall temperature and compared to our experimental correlation (11) over the complete range $10\,000 \leqslant Re_j \leqslant 30\,000$, $3 \leqslant R/D \leqslant 10$ and $2 \leqslant H/D \leqslant 6$, leading to an average relative deviation of 7%, with a maximum relative deviation of 15% obtained for low average Nusselt numbers.

Due to the boundary layer development along the wall past the stagnation point, the gas-to-wall temperature difference influences the average Nusselt number, via the viscosity dependence on temperature. This effect has been investigated with the numerical model, and the experimental correlation can be corrected by introducing a viscosity ratio $(\mu_j/\mu_w)^n$. Then a general correlation (22) has been proposed for jet impingement heat transfer calculations at a uniform wall temperature, for $10\,000 \leqslant Re_j \leqslant 30\,000$, $3 \leqslant R/D \leqslant 10$, $2 \leqslant H/D \leqslant 6$ and $1.1 \leqslant \mu_j/\mu_w \leqslant 1.4$. The average Nusselt number increases with the jet Reynolds number, decreases with the plate radius but has only a little dependency on both the nozzle-to-plate distance and gas-to-wall temperature difference.

It should be noted that the proposed correlation (22) can be utilised for free impinging jet heat transfer calculation, as the numerical results have confirmed that the enclosure diameter chosen in the experimental set-up was large enough to neglect any confinement effect on the mean heat transfer. This correlation (22) is thus thought to be applicable in many engineering configurations requiring the evaluation of impinging jet heat transfer coefficients.

References

[1] D. Lytle, B.W. Webb, Air jet impingement heat transfer at low nozzle-plate spacings, Int. J. Heat Mass Transfer 37 (12) (1994) 1687–1697.
[2] M. Fenot, J.-J. Vullierme, E. Dorignac, Local heat transfer due to several configurations of circular air jets impinging on a flat plate with and without semi-confinement, Int. J. Thermal Sciences 44 (2005) 665–675.
[3] D.H. Lee, S.Y. Won, Y.T. Kim, Y.S. Chung, Turbulent heat transfer from a flat surface to a swirling round impinging jet, Int. J. Heat Mass Transfer 45 (2002) 223–227.
[4] N. Gao, H. Sun, D. Ewing, Heat transfer to impinging round jets with triangular tabs, Int. J. Heat Mass Transfer 46 (2003) 2557–2569.
[5] N. Gao, D. Ewing, Investigation of the effect of confinement on the heat transfer to round impinging jets exiting a long pipe, Int. J. Heat Fluid Flow 27 (2006) 33–41.
[6] C.J. Hoogendoorn, The effect of turbulence on heat transfer at a stagnation point, Int. J. Heat Mass Transfer 20 (1977) 1333–1338.
[7] D.W. Zhou, O. Sang-Joon Lee, Forced convective heat transfer with impinging rectangular jets, Int. J. Heat Mass Transfer 50 (2007) 1916–1926.
[8] G.W. Lowery, R.I. Vachon, The effect of turbulence on heat transfer from heated cylinders, Int. J. Heat Mass Transfer 18 (1975) 1229–1242.

[9] C. Gau, I.C. Lee, Flow and impingement cooling heat transfer along triangular rib-roughened walls, Int. J. Heat Mass Transfer 43 (2000) 4405–4418.
[10] F. Mathey, Heat transfer modeling, Journées utilisateurs FLUENT, Paris, 12 oct. 2005.
[11] E.E.M. Olsson, L.M. Ahrné, A.C. Trägårdh, Heat transfer from a slot air jet impinging on a circular cylinder, J. Food Engineering 63 (2004) 393–401.
[12] S.O. Akansu, Heat transfers and pressure drops for porous-ring turbulators in a circular pipe, Applied Energy 83 (2006) 280–298.
[13] J.W. Baughn, A.E. Hechanova, X. Yan, An experimental study of entrainment effect on the heat transfer from a flat surface to a heated circular impinging jet, J. Heat Transfer 113 (1991) 1023–1025.
[14] FLUENT 6.2 user's guide. Fluent Incorporated, Centerra Resource Park, 10, Cavendish Court, Lebanon (NH) 03766, USA, 2005.
[15] S. Whitaker, Fundamental Principles of Heat Transfer, Pergamon Press Inc., 1977.
[16] J.H. Lienhard IV, J.H. Lienhard V, A Heat Transfer Textbook, Phlogiston Press, 2003.